

# Synthesis and characterization of $\alpha$ -mangostin imprinted polymers and its application for solid phase extraction

Neena Zakia<sup>1,2a</sup>, Muhammad A. Zulfikar<sup>1b</sup> and Muhammad B. Amran<sup>\*1</sup>

<sup>1</sup> Analytical Chemistry Research Group, Institut Teknologi Bandung,  
Jalan Ganesha No 10, Bandung, 40132, Indonesia

<sup>2</sup> Department of Chemistry, Universitas Negeri Malang, Jalan Semarang No 5, Malang, 65145, Indonesia

(Received May 22, 2020, Revised October 9, 2020, Accepted October 22, 2020)

**Abstract.**  $\alpha$ -mangostin imprinted polymers have been synthesized by a non-covalent imprinting approach with  $\alpha$ -mangostin as a template molecule. The  $\alpha$ -mangostin molecularly imprinted polymers (MIPs) prepared by radical polymerization using methacrylic acid, ethylene glycol dimethacrylate, benzoyl peroxide, and acetonitrile, as a monomer, crosslinker, initiator, and porogen, respectively. The template was removed by using methanol:acetic acid 90:10 (v/v). The physical characteristics of the polymers were investigated by Fourier Transform Infrared spectroscopy (FTIR), scanning electron microscopy (SEM), and thermogravimetric analysis (TGA). The rebinding studies were carried out by batch methods. The results exhibited that the MIPs was able to adsorb the  $\alpha$ -mangostin at pH 2 and the contact time of 180 min. The kinetic adsorption data of  $\alpha$ -mangostin performed the pseudo-second order model and followed the Langmuir isotherm model with the adsorption capacity of 16.19 mg.g<sup>-1</sup>. MIPs applied as a sorbent material in solid-phase extraction, namely molecularly imprinted solid-phase extraction (MISPE) and it shows the ability for enrichment and clean-up of  $\alpha$ -mangostin from the complex matrix in medicinal herbal product and crude extract of mangosteen (*Garcinia mangostana* L.) pericarp. Both samples, respectively, which were spiked with  $\alpha$ -mangostin gives recovery more than 90% after through by MISPE in all concentration ranges.

**Keywords:**  $\alpha$ -mangostin; molecularly imprinted polymers; solid phase extraction; enrichment; clean-up

## 1. Introduction

$\alpha$ -Mangostin found in mangosteen (*Garcinia mangostana* L.) pericarp which has pharmacological bioactive properties is able to treat many diseases.  $\alpha$ -Mangostin compound is a prenylated xanthone derivatives at positions 2 and 8, a hydroxy groups at atom C1, C3, and C6, a methoxy group at atom C7, and an oxo group at atom C9. The chemical structure of  $\alpha$ -mangostin is shown in Fig. 1.

The health benefit of  $\alpha$ -mangostin has been reported by many research studies.  $\alpha$ -Mangostin have activities as antioxidant, anticancer, antitumor, and anti-inflammatory (Fabiola and Mark 2013, Apinya *et al.* 2009, Kenji *et al.* 2004, Abdalrahim *et al.* 2012). In order to use  $\alpha$ -mangostin as an active molecule, extraction of  $\alpha$ -mangostin is a crucial step.

\*Corresponding author, Professor, E-mail: [amran@chem.itb.ac.id](mailto:amran@chem.itb.ac.id)

<sup>a</sup> Doctoral Student, E-mail: [neena.zakia.fmipa@um.ac.id](mailto:neena.zakia.fmipa@um.ac.id)

<sup>b</sup> Ph.D., E-mail: [zulfikar@chem.itb.ac.id](mailto:zulfikar@chem.itb.ac.id)

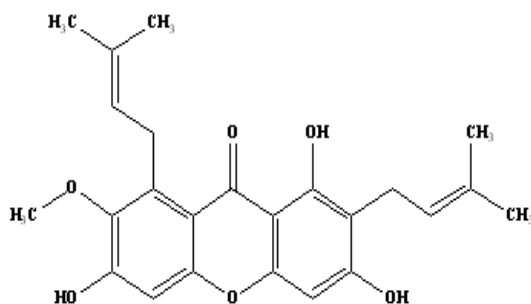


Fig. 1 Chemical structure of  $\alpha$ -mangostin

Several pretreatment techniques for  $\alpha$ -mangostin prior to the analysis that have been studied are chromatography using silica gel (Mohamed *et al.* 2014), liquid chromatography (Abdalahim *et al.* 2012), solvent extraction (Pothitirat and Gritsanapan 2009, Eukun Sage *et al.* 2018) and solid phase extraction (Mughtaridi *et al.* 2017). Compared with solvent extraction, solid phase extraction (SPE) gives a more advantages that is simple, low time-consuming, less solvent consumption, and give better pre-concentrated. However, sorbents in SPE cartridge such a C-18 or silica have the disadvantage of lack selectivity and specificity, and low recovery for target molecules. Currently, molecularly imprinted polymers have been recognized as useful sorbent materials for SPE for extraction, purification, and enrichment purpose (Tamayo *et al.* 2007, Qiao *et al.* 2006, Maria *et al.* 2012).

Molecularly imprinted polymers are the synthetic polymer which provide the ability to recognize and bind specific toward the template molecule (Karsten 2001). By interaction between template and functional monomer to form the complex before polymerization by covalent or non-covalent bonding (Caro *et al.* 2006), and combined with a crosslinker and an initiator in appropriate porogen, the imprinting polymer will be produced. Non-covalent imprinting approach occurred due to interactions between functional monomer and template molecule through hydrogen bonds or hydrophobic interaction (Martin-Esteban *et al.* 2001). After removal the template from the polymers, it will be generates selective cavities (Maria *et al.* 2012, Geng *et al.* 2016). Molecularly imprinted polymers were widely used as SPE technique for the selective extraction and pre-concentration of the analytes in complex samples, that namely molecularly imprinted solid-phase extraction (MISPE) (Tamayo *et al.* 2007).

In this work, we present the development of molecularly imprinted polymers for the rapid analysis of  $\alpha$ -mangostin and its application as stationary phase in solid phase extraction.  $\alpha$ -Mangostin imprinted polymers prepared by radical polymerization using a non-covalent imprinting approach with  $\alpha$ -mangostin as the template molecule, methacrylic acid as a monomer, ethylene glycol dimethacrylate as a crosslinker, benzoyl peroxide as an initiator, and acetonitrile as a porogen. The template was removed by soxhlet extraction using methanol:acetic acid 90:10 (v/v) to generate the specific recognition cavities. For further, the term of MIPs is used to refer to  $\alpha$ -mangostin imprinted polymers. Non-imprinted polymers (NIPs) was synthesized following the same procedure in the absence of template. Polymer characterization and rebinding studies of MIPs and NIPs materials were evaluated to obtain the optimization of the polymers. The binding assays have been determined using high-performance liquid chromatography (HPLC). A MISPE method has been carried out for  $\alpha$ -mangostin in medicinal herbal product and crude extract of mangosteen (*Garcinia mangostana* L.) pericarp. There has been no report about MISPE for  $\alpha$ -mangostin.

## 2. Experimental

### 2.1 Materials

The materials used in this study were methacrylic acid (Merck), benzoyl peroxide (Merck), acetonitrile (Merck), methanol (Merck), and acetic acid (Merck), ethylene glycol dimethacrylate (Aldrich),  $\alpha$ -mangostin (98%, ChengDu, China), and distilled water. Nitrogen gas was purchased from a local supplier. Medicinal herbal product and mangosteen fruit were purchased from a local supermarket in Bandung (West Java, Indonesia).

### 2.2 Synthesis of $\alpha$ -mangostin imprinted polymers

The molecularly imprinted polymers were prepared by radical polymerization.  $\alpha$ -mangostin imprinted polymers were synthesized by using methacrylic acid (MAA) as a functional monomer, ethylene glycol dimethacrylate (EGDMA) as a crosslinker, benzoyl peroxide (BPO) as an initiator, and acetonitrile as a porogenic solvent.  $\alpha$ -mangostin (0.5 mmol) was dissolved in acetonitrile (20 mL) containing of MAA (2 mmol) in a thick-wall glass tube. The solution was stirred at room temperature (150 rpm) for 24 hours in order to prepolymerization process. After that 10 mmol EGDMA was added into the solution. Nitrogen was purged for 5 min and then added 2% BPO initiator. The mixture is completely degas for 5 min. The polymerization was performed by incubating the mixture in oil bath at 60°C for 8 hours. The resulted polymers were extracted  $\alpha$ -mangostin as a template using soxhlet apparatus for 48 hours in methanol:acetic acid (90:10, v/v). Quantitative removal of the template was ensured by monitoring the amount of template remaining by High Performance Liquid Chromatography HPLC (Infinity Agilent Tech 1260 Series with DAD detector, and Phenomenex LC column Gemini 5 $\mu$  C18 110 A 150  $\times$  4.6 mm) at wavelength of 316 nm. The absorption spectra of  $\alpha$ -mangostin solutions was investigated by UV-Vis spectrophotometer (UV-Vis Spectrometry Agilent Technologies HP 8453). The imprinted polymers formed were crushed and sieved into 60 mesh, then dried in an oven at 55°C. The MIPs were stored at room temperature for further experiments. Control polymers (non imprinted polymers or NIPs) follows the steps of synthesis MIPs without the presence of  $\alpha$ -mangostin molecule.

### 2.3 Physical characterization

The functional groups of molecularly imprinted polymers (MIPs) and non imprinted polymers (NIPs) were characterized using Fourier Transformation Infra-Red Spectrometry (FTIR Prestige 21 Shimadzu) in the wavenumber 4000-400  $\text{cm}^{-1}$ . Surface morphology of MIPs and NIPs were studied by Scanning Electron Microscopy-Energy Dispersive X-Ray (SEM-EDX FEI type INSPECT-S50). The effects of thermal stability of MIPs and NIPs were observed using a thermogravimetric analysis (STA LINSEIS PT1600).

### 2.4 Batch rebinding, kinetic, and isotherm adsorption studies

Batch binding analysis was examined to evaluate of adsorption capacity of synthesized polymers. Binding analysis was carried out by to analyze of effect of pH, interaction time, and optimum adsorption capacity.

#### 2.4.1 Effect of pH

10 mg of MIPs and NIPs particles respectively, were placed in vial and then incubated with 5 mL of  $\alpha$ -mangostin 25 mg.L<sup>-1</sup> in methanol:water 1:1 for 24 hours in 150 rpm at a pH range of 2 to 8. The filtrate was separated from the sorbent, and measured by HPLC using a mixture of methanol:water 95:5 (v/v) as a mobile phase with flow rate 1 mL per min. The amount of  $\alpha$ -mangostin bound to polymer was calculated using Eq. (1).

$$q_e = \frac{v(C_i - C_e)}{w} \quad (1)$$

where  $q_e$  is the adsorption capacity (mg.g<sup>-1</sup>),  $v$  is the volume of solution (L),  $C_i$  and  $C_e$  are the initial concentration and the final concentration of  $\alpha$ -mangostin (mg.L<sup>-1</sup>), respectively, and  $w$  is the sorbent mass (g).

#### 2.4.2 Effect of interaction time

10 mg of MIPs particles were placed in vial and then interacted with 5 mL of  $\alpha$ -mangostin 25 mg.L<sup>-1</sup> in methanol:water 1:1 (v/v) at optimum pH in 150 rpm with a time variation of 10-180 minutes. The filtrate was separated from the sorbent, and measured by HPLC using a mixture of methanol:water 95:5 (v/v) as a mobile phase with flow rate 1 mL per min.

#### 2.4.3 Evaluation of the adsorption characteristics

The binding capacity of the polymers were performed by incubating 10 mg of MIPs in 5 mL volume of  $\alpha$ -mangostin in several concentration (10 to 150 mg.L<sup>-1</sup>) in a vial at the optimum pH and the optimum time. The solution were then analyzed by HPLC using a mixture of methanol:water 95:5 (v/v) as a mobile phase with flow rate 1 mL per min. The same procedure was also carried out for NIPs. The adsorption capacity was determined by using Langmuir and Freundlich isotherms.

### 2.5 Application of MIPs for solid phase extraction (SPE) system

#### 2.5.1 Optimization of solid phase extraction (SPE) system

50 mg of MIPs particles were dry packed in 1 mL cartridge using Supelco Visitreptm<sup>24</sup> SPE, and namely as MISPE. Equilibration of the column, loading and washing were performed using 1 mL aliquots of the corresponding solutions and elution of the retained analytes with different elution solvents (methanol:water 95:5 (v/v), methanol:acetic acid 75:25 (v/v), and methanol:acetic acid 90:10 (v/v)). The collected fractions were analyzed by HPLC using a mixture of methanol:water 95:5 (v/v) as a mobile phase with flow rate 1 mL per min.

#### 2.5.2 Application of MIPs for extraction of $\alpha$ -mangostin from medicinal herbal product and crude extract of mangosteen (*Garcinia mangostana* L.) pericarp

150 mg of medicinal herbal product were prepared by extracting in 10 mL of methanol:water 1:1 (v/v) pH 2.1 mL of sample extracts was applied to MISPE system at a constant flow rate 0.20 mL min<sup>-1</sup> with the aid of vacuum pump. The SPE system was conditioned with methanol and equilibrated with methanol:water 1:1 (v/v) pH 2, washed with water, and eluted with 500  $\mu$ L methanol:acetic acid 90:10 (v/v). The elution fraction then analyzed by HPLC using a mixture of methanol:water 95:5 (v/v) as a mobile phase with flow rate 1 mL per min. The crude extract of mangosteen (*Garcinia mangostana* L.) pericarp were also treated the same as a medicinal herbal product.

For quantification purposes, in the recovery experiments, aliquots of medicinal herbal product and crude extract of mangosteen pericarp, respectively, were spiked with 60 mg.L<sup>-1</sup> and 80 mg.L<sup>-1</sup> of  $\alpha$ -mangostin in methanol:water 1:1 (v/v) pH 2. The spiked sample (1 mL) then applied to MISPE that has been conditioned with methanol and equilibrated with methanol:water 1:1 (v/v) pH 2. The washing step was carried out with water and eluted with 500  $\mu$ L methanol:acetic acid 90:10 (v/v) for pre-concentrated in the MIP column. The elution fraction then detected by HPLC using a mixture of methanol:water 95:5 (v/v) as a mobile phase with flow rate 1 mL per min. The recovery percentage of the elution fraction was then calculated.

### 3. Results and discussion

#### 3.1 Physical characterization of sorbents

##### 3.1.1 FTIR Spectroscopy

FTIR analysis was used to investigate the functional groups in MIPs and NIPs particles (Fig. 2). The MIPs before leaching spectra appeared absorption bands at 3468, 2992, 1728, 1638, 1447, and 1165 cm<sup>-1</sup> can be assigned to the stretching vibration of hydroxyl (O-H) groups, -C-H bonds on methyl groups, C=O bonds on carbonyl groups, C=C bonds, CH<sub>3</sub> bending, and C-O stretching vibration, respectively (Jin *et al.* 2013).

The broad band at 3468 cm<sup>-1</sup> indicates that hydrogen bond occurs between the functional monomer (MAA) and template molecule ( $\alpha$ -mangostin), that confirmed with the complex of template-monomer-spectra in prepolymerization step. A significant band at 1728 and 1165 cm<sup>-1</sup> in spectra of MIPs before leaching were the characteristic peaks of EGDMA, which confirm that the crosslinker and the functional monomer polymerized. Thus, these spectra suggesting that the MIPs was synthesized successfully.

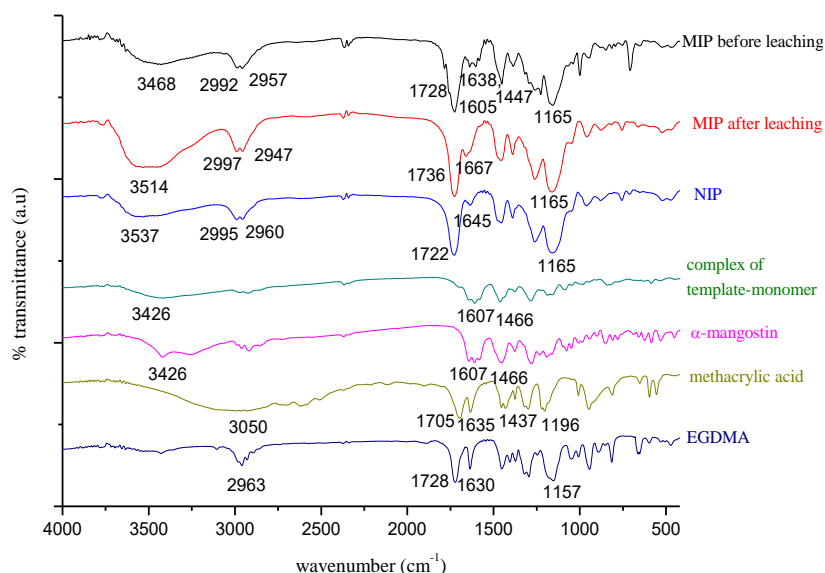
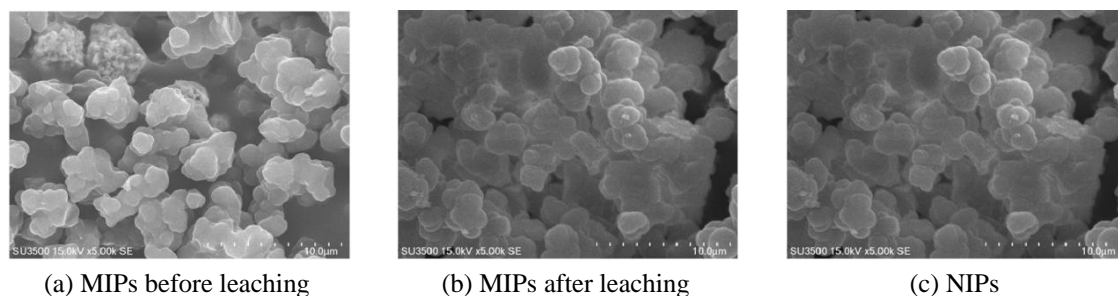


Fig. 2 FTIR spectra of MIP particles before and after template removal, NIP particles, complex of template-monomer,  $\alpha$ -mangostin, methacrylic acid, and ethylene glycol dimethacrylate (EGDMA)



(a) MIPs before leaching (b) MIPs after leaching (c) NIPs

Fig. 3 SEM images of MIPs particles before and after template removal and NIPs particles

On the other hand, spectra of MIPs after leaching and NIPs are approximately similar. The change of IR spectrum of the MIPs before and after template removal were shown by shifting the wavenumber of some functional groups. The peak at  $1607\text{ cm}^{-1}$  in MIPs before leaching spectra correspond to C=C stretching vibration of template, which was not found in the MIPs spectrum after leaching. It was confirmed that the template has been removal after extraction process.

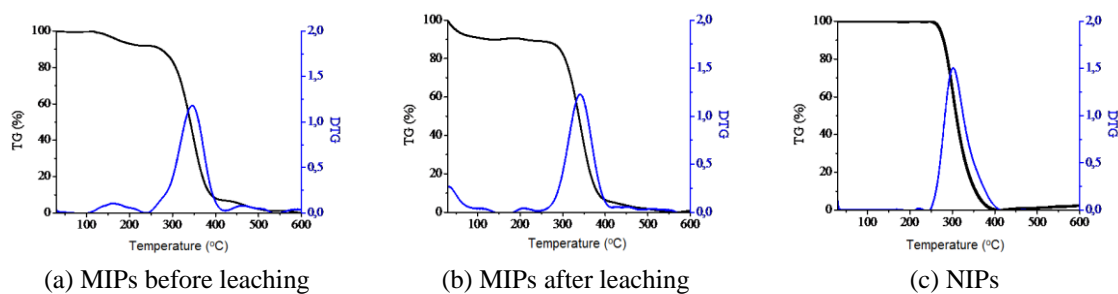
### 3.1.2 Scanning electron microscopy (SEM)

The polymer particles morphology were investigated using a scanning electron microscopy (SEM). The measurement result of SEM of MIPs before and after leaching, and NIPs were shown in Fig. 3.

From SEM image showed the polymer particles have irregular shape and sizes due to the grinding process. MIPs after leaching was more hollow than MIPs before leaching, due to the template of MIPs before leaching was successfully removed and formed the cavity as seen in MIPs after leaching. Particles shape of NIPs looked smaller than MIPs particles, due to absence the template.

### 3.1.3 Thermal analysis

Effect of thermal stability of MIPs and NIPs were performed using thermogravimetric analysis (TGA). Results of TGA analysis was shown in Fig. 4. From the thermogram curve were performed that the polymers have thermal stability up to  $100^\circ\text{C}$ . MIPs before leaching has several decomposition steps at temperatures between  $103\text{-}232^\circ\text{C}$ ,  $245\text{-}422^\circ\text{C}$ ,  $422\text{-}535^\circ\text{C}$ , and above  $560^\circ\text{C}$ . In MIPs after leaching was obtained three steps which show the difference with the MIPs before leaching, due to the mass loss of template molecule. For NIPs material, the polymer is thermally stable to  $247^\circ\text{C}$ . Temperature before  $247^\circ\text{C}$  there is no change in mass. From the curve, the biggest



(a) MIPs before leaching (b) MIPs after leaching (c) NIPs

Fig. 4 TGA curve of MIPs particles before and after template removal, and NIPs particles

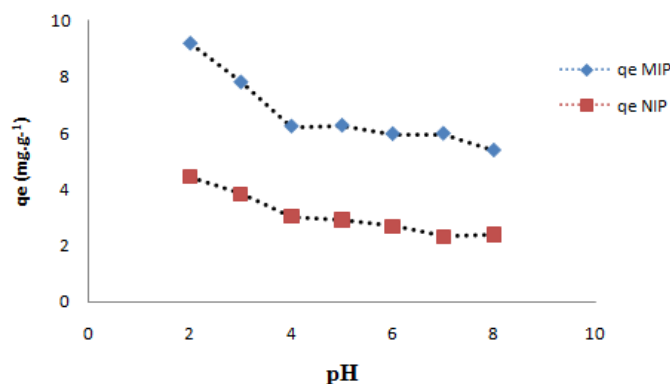


Fig. 5 Adsorption capacity of  $\alpha$ -mangostin adsorbed on MIPs and NIPs as function of pH

mass reduction in all materials occurred in temperature range between 243-417°C around 84% corresponds to decomposition of polymer constituent such as crosslinker and initiator. Significant differences were shown in MIPs before and after leaching, that in MIPs before occurred mass loss at 422-535°C and above 568°C were indicated decomposition of  $\alpha$ -mangostin. MIPs after leaching has only a slight mass loss at 417-490°C and above 520°C more stable. The thermogram curve of MIPs after leaching and NIPs have similarity, this indicates that the leaching process of template molecule has been successful. All materials were completely decomposed prior to reach the temperature of 560°C.

### 3.2 Rebinding study

#### 3.2.1 Effect of pH

The effect of pH on the sorption of  $\alpha$ -mangostin was investigated by varying the solution pH from 2 to 8. The pH influence on adsorption of  $\alpha$ -mangostin on MIPs and NIPs shown in Fig. 5. According to Fig. 5, the binding amount of  $\alpha$ -mangostin that adsorbed in MIPs gradually decreases with the increasing pH.

The highest binding capacity of  $\alpha$ -mangostin reached at pH 2. Since the  $pK_{a1}$  value of the  $\alpha$ -mangostin is 3.89, wherein pH less than  $pK_a$  the compound can be protonated therefore the adsorption between the MIPs and  $\alpha$ -mangostin molecule occurs through the interaction of hydrogen bonds. Above pH 4, the  $\alpha$ -mangostin molecules deprotonated thus the binding capacity decreased (Nor *et al.* 2013).

#### 3.2.2 Effect of interaction time

The effect of the interaction time on adsorption of  $\alpha$ -mangostin is given in Fig. 6. The binding process in the initial stage exhibit quickly and then the adsorption rate slowed down gradually with increasing contact time. In the initial stage, the MIPs have enough of unoccupied imprinted cavities, the template molecules can be easily taken up by the cavities on polymer. However in the increasing time, the cavities decreases thus the amount adsorbed tends not to increase significantly.

The interaction time optimum of  $\alpha$ -mangostin adsorption was reached in 180 min and the adsorbed amount on MIPs was 7.17 mg.g<sup>-1</sup>. The kinetics study of adsorption were analyzed using Lagergren pseudo-first order model and pseudo-second order model (Jean-Pierre 2016, Ho and McKay 1999, Hamou *et al.* 2018). The pseudo-first order and pseudo-second order kinetic models

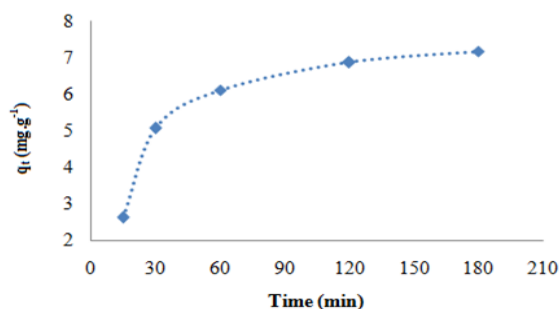


Fig. 6 The effect of interaction time with adsorption capacity ( $q_e$ ) on MIPs

is shown in Eqs. (2) and (3), respectively, were used to fit the experimental data

$$\ln(q_e - q_t) = \ln(q_e) - k_1 t \quad (2)$$

$$\frac{t}{q_t} = \frac{1}{k_2 q_e^2} + \frac{t}{q_e} \quad (3)$$

where  $q_e$  ( $\text{mg.g}^{-1}$ ) is the amount of adsorption at equilibrium,  $q_t$  ( $\text{mg.g}^{-1}$ ) denotes the amount of adsorption at time  $t$  (min),  $k_1$  ( $\text{min}^{-1}$ ) is the rate constant of pseudo-first order adsorption, and  $k_2$  ( $\text{g.mg}^{-1}.\text{min}^{-1}$ ) is the pseudo-second order rate constants of adsorption.

The kinetics adsorption curves are shown in Fig. 7 and the kinetic parameters are presented in Table 1.

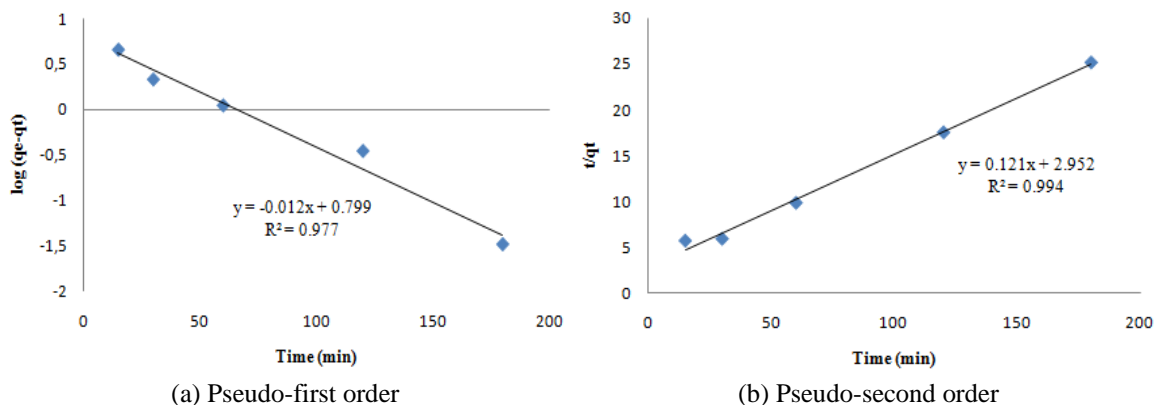


Fig. 7 Kinetic curve of  $\alpha$ -mangostin adsorption on MIPs

Table 1 Kinetic data for adsorption of  $\alpha$ -mangostin on MIPs

Model	$q_e$ exp (mg/g)	$q_e$ cal (mg/g)	$k_1$	$k_2$	$R^2$
Pseudo-first order	7.17	3.35	0.263	-	0.977
Pseudo-second order	7.17	8.20	-	0.005	0.994



From the calculated results were obtained that the values of correlation coefficient ( $R^2$ ) of pseudo-second order model for MIPs are higher than those for the pseudo-first model. The calculated equilibrium adsorption capacity ( $q_e$  cal) values close to the experimental data ( $q_e$  exp) in the pseudo-second order model. Based on the results can be concluded that the pseudo-second order model was more suitable than the pseudo-first order to describe the adsorption kinetics of  $\alpha$ -mangostin on MIPs.

The rate-limiting step is pseudo-second order which involves specific molecular interactions between  $\alpha$ -mangostin compounds and functional groups in imprinted molecular cavities. These results can be used to exhibit that the synthesized MIPs have requirements for use as a SPE sorbent. In addition, from the reaction kinetics that is followed, it can be used to indicate whether there are specific cavities in the polymer.

### 3.2.3 Evaluation of the adsorption characteristics

In this study, the binding capacity of the polymers has been evaluated in equilibrium rebinding batch experiment. The experiment was carried out by varying the initial concentration of  $\alpha$ -mangostin. Fig. 8 shows the binding capacity of MIPs and NIPs for  $\alpha$ -mangostin, which is an adsorption capacity ( $q_e$ ) on MIPs and NIPs versus initial concentration ( $C_i$ ) of  $\alpha$ -mangostin.

It was observed that the binding capacity of  $\alpha$ -mangostin increases with the increases of initial concentration of  $\alpha$ -mangostin and reached adsorption equilibrium. The results indicate that the MIPs was reaching saturation at higher concentrations. The amount of  $\alpha$ -mangostin bound to the MIPs is higher than on the NIPs, proving that imprinted site on the MIPs have specific binding sites for the template molecule. Adsorption isotherms were evaluated using Langmuir and Freundlich model isotherms (Nimibofa *et al.* 2017, Claudio *et al.* 2004, Robert *et al.* 2001). The binding isotherms showed a good fitting to the Langmuir model from the coefficient correlation value. The fitting results are given in Table 2 and Fig. 9.

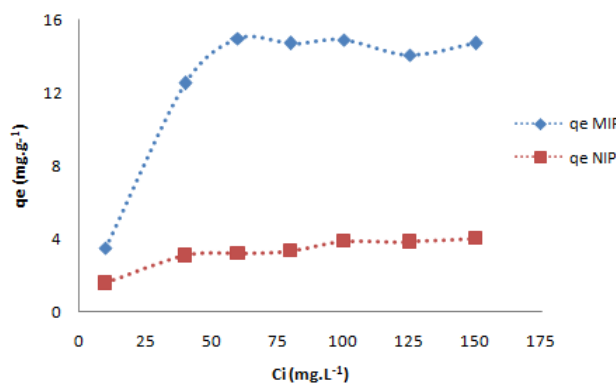


Fig. 8 Adsorption capacity of various concentration of  $\alpha$ -mangostin on MIPs and NIPs

Table 2 The fitting results of Langmuir and Freundlich model parameters for MIPs and NIPs

Polymer	Langmuir model			Freundlich model		
	$Q_{max}$ (mg.g <sup>-1</sup> )	$K_L$ (L.mg <sup>-1</sup> )	$R^2$	n	$K_F$ (L.g <sup>-1</sup> )	$R^2$
MIPs	16.19	0.16	0.953	0.27	4.46	0.789
NIPs	4.22	0.08	0.986	0.27	1.06	0.982

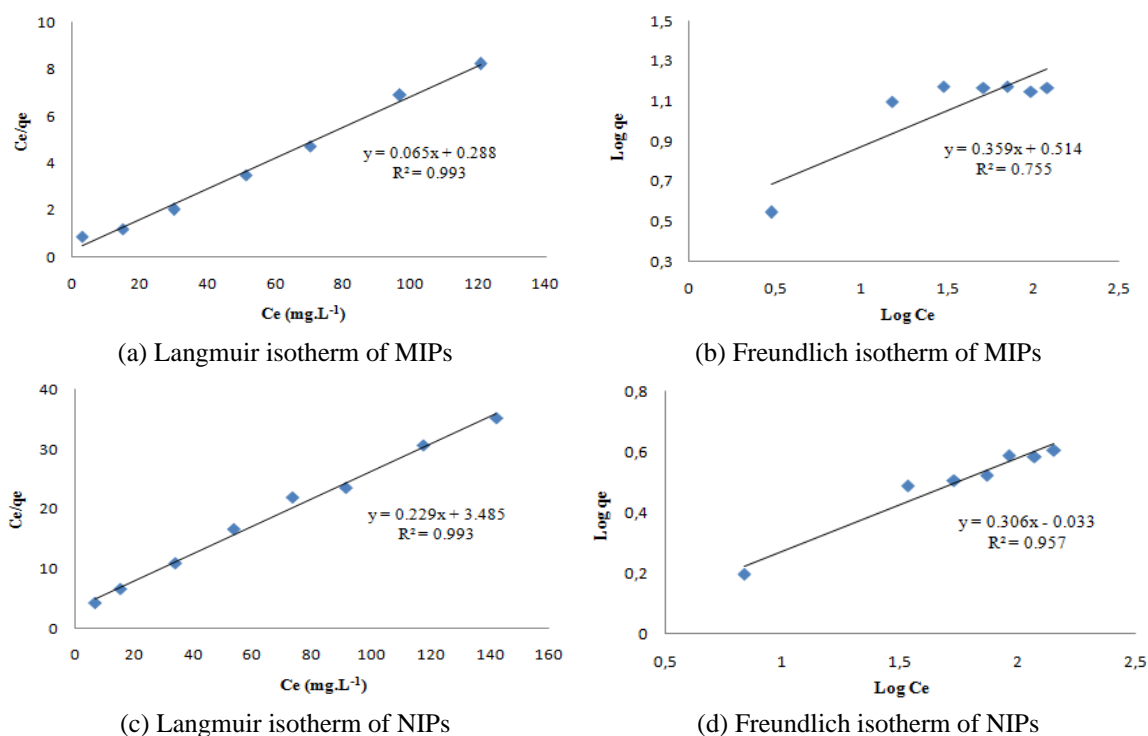


Fig. 9 Langmuir and Freundlich plots for adsorption of  $\alpha$ -mangostin on MIPs and NIPs

The Langmuir and Freundlich model isotherms to estimate the phenomenon of adsorption of  $\alpha$ -mangostin on the sorbent surface. In this study, the isotherm model is following Langmuir model, which suggested that the adsorption process are monolayer adsorption. It is important to know that by following the Langmuir model, the sorbent specificity is better due to the specific binding sites of the MIPs are more homogeneous, thus for SPE applications are preferred.

### 3.3 Application of MIPs for solid phase extraction (SPE) system

#### 3.3.1 Optimization of solid phase extraction (SPE) system

The MIPs was applied as the sorbent of the SPE cartridge for removal of potential interferents and preconcentration  $\alpha$ -mangostin in herbal product (Esther and Antonio 2010). In order to find the optimum conditions for eluent on the MISPE column, several of solvents were used to obtain recovery of analyte quantitatively. The results of elution solvent for recovery the  $\alpha$ -mangostin are given in Fig. 10.

From Fig. 10, we found that methanol:acetic acid 75:25 (v/v) was the best elution solvent. The recovery was achieved 95.41%, that suggested the elution solvent can be disrupt the hydrogen bonding between  $\alpha$ -mangostin and active site in the cavities of imprinted polymers (Martín-Esteban 2001). However, in the further work, methanol:acetic acid 90:10 (v/v) was used due to this solvent does not damage the imprinted polymers and the HPLC column in its analysis, and the percent recovery is almost equal to methanol:acetic acid 75:25 (v/v), which is 94.53%.

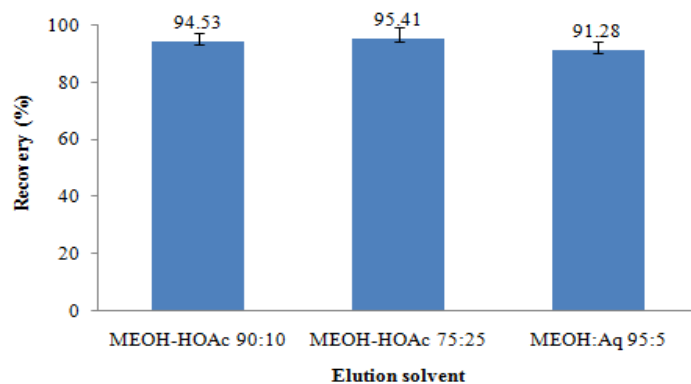


Fig. 10 Recovery percentage of elution solvent condition

### 3.3.2 Application of MIPs for extraction of $\alpha$ -mangostin from medicinal herbal and crude extracts of mangosteen (*Garcinia mangostana* L.) pericarp

In order to evaluate the performance of the MISPE method, a medicinal herbal product and crude extract of mangosteen pericarp that contain  $\alpha$ -mangostin were carried out using the optimized protocol. The developed procedure was applied to the enrichment and clean-up of  $\alpha$ -mangostin in sample extracts. After MISPE, the sample extracts were analysed and the results shown in Fig. 11. The chromatograms exhibited the MISPE performance of sample extracts before and after going through MISPE to clean-up and enrichment process for  $\alpha$ -mangostin, that the retention time for  $\alpha$ -mangostin was  $3.75 \pm 0.10$  min. The matrix compounds in the sample extract was considerably reduced with MISPE. From the chromatograms indicated that MISPE capable produced an enrichment process.

Medicinal herbal sample were spiked in 60 and 80  $\text{mg.L}^{-1}$  concentration of  $\alpha$ -mangostin, that gives recoveries 99.67 and 107.27%, respectively. Crude extract of mangosteen pericarp sample which were spiked with 60 and 80  $\text{mg.L}^{-1}$  concentration of  $\alpha$ -mangostin gives recovery 93.35

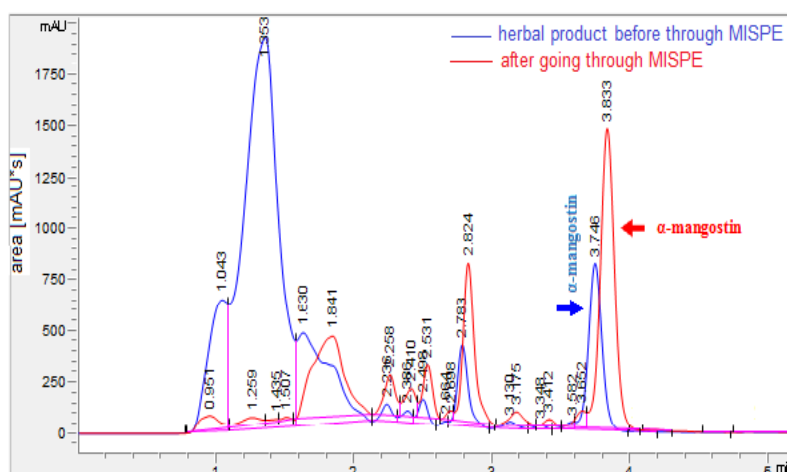


Fig. 11 Chromatograms of an herbal extract before through the MISPE (blue line) and after through the MISPE (red line) which clean-up and enrichment of sample was happened

and 93.38%, respectively. It suggested that the MISPE was successfully developed to enrich and clean up the matrix compounds in sample extract. The cartridges have been used more than 10 times without losing their recognition properties.

#### 4. Conclusions

$\alpha$ -Mangostin imprinted polymers have been successfully synthesized by radical polymerization with non-covalent approach. Adsorption of  $\alpha$ -mangostin on MIPs was obtained at pH 2 and at 180 min of interaction time. In the kinetic study, it was exhibited that adsorption followed the kinetic model of pseudo-second order. The adsorption process obeys a Langmuir adsorption isotherm with the adsorption capacity is 16.19 mg.g<sup>-1</sup>. The fabricated  $\alpha$ -mangostin imprinted polymers has potential use as a sorbent in solid phase extraction (SPE) for removal the interferents of complex matrices and preconcentration process. Further, the novel MIPs developed as alternative for traditional SPE sorbents for analytical purposes in many fields such as in food, agricultural, health, and pharmaceutical.

#### Acknowledgments

The research described in this paper was financially supported the Research, Technology, and Higher Education Ministry Indonesia for Doctoral Dissertation Research (PDD) Grant 2019.

#### References

- Abdalahim, F.A.A., Khalid, M.A., Zhari, I. and Amin, M.S.A.M. (2012), "In vitro and in vivo anti-colon cancer effects of *Garcinia mangostana* xanthenes extract", *BMC Complement Altern. Med.*, **12**(104), 1-10. <https://doi.org/10.1186/1472-6882-12-104>
- Apinya, C., Yaowaluk, M., Arusa, C., Amornmart, J., Panomwan, P., Piniti, R. and Sunit, S. (2009), "Prenylated xanthone composition of *Garcinia mangostana* (mangosteen) fruit hull", *Chromatographia*, **69**, 315-318. <https://doi.org/10.1365/s10337-008-0890-1>
- Caro, E., Marcé, R.M., Borrull, F., Cormack, P.A.G. and Sherrington, D.C. (2006), "Application of molecularly imprinted polymers to solid-phase extraction of compounds from environmental and biological samples", *Trends Anal. Chem.*, **25**(2), 143-154. <https://doi.org/10.1016/j.trac.2005.05.008>
- Claudio, B., Gianfranco, G., Christina, G., Cinzia, T. and Laura, A. (2004), "Adsorption isotherms of a molecular imprinted polymer prepared in the presence of a polymerisable template indirect evidence of the formation of template clusters in the binding site", *Anal. Chim. Acta*, **504**(1), 43-52. [https://doi.org/10.1016/S0003-2670\(03\)00671-8](https://doi.org/10.1016/S0003-2670(03)00671-8)
- Esther, T. and Antonio, M-E. (2010), "Molecularly imprinted polymers for sample preparation: a review", *Anal. Chim. Acta*, **668**(2), 87-99. <https://doi.org/10.1016/j.aca.2010.04.019>
- Eukun Sage, E., Jailani, N., Md. Taib, A.Z., Mohd Noor, N., Mohd Said, M.I., Abu Bakar, M. and Mackeen, M.M. (2018), "From the front or back door? quantitative analysis of direct and indirect extractions of  $\alpha$ -mangostin from mangosteen (*Garcinia mangostana*)", *PloS One*, **13**(10), 1-12. <https://doi.org/10.1371/journal.pone.0205753>
- Fabiola, G-O. and Mark, L.F. (2013), "Biological activities and bioavailability of mangosteen xanthenes: a critical review of the current evidence", *Nutrients*, **5**(8), 3163-3183. <https://doi.org/10.3390/nu5083163>
- Geng, N.W., Kun, Y., Hui, Z.L., Meng, X.F. and Jian, P.W. (2016), "Molecularly imprinted polymer-based

- solid phase extraction combined high performance liquid chromatography for determination of fluoroquinolones in milk”, *Anal. Methods*, **8**(27), 5511-5518. <https://doi.org/10.1039/C6AY00810K>
- Hamou, M., Hammou, A., Mustapha, A. and Hamid, M. (2018), “Critical of linear and nonlinear equations of pseudo-first order and pseudo-second order kinetic models”, *KIJOMS*, **4**(2), 244-254. <https://doi.org/10.1016/j.kijoms.2018.04.001>
- Ho, Y.S. and McKay, G. (1999), “Pseudo-second order model for sorption processes”, *Process Biochem*, **34**(5), 451-465. [https://doi.org/10.1016/S0032-9592\(98\)00112-5](https://doi.org/10.1016/S0032-9592(98)00112-5)
- Jean-Pierre, S. (2016), “On the comparison of pseudo-first order and pseudo-second order rate laws in the modeling of adsorption kinetics”, *Chem. Eng. J.*, **300**, 254-263. <http://dx.doi.org/10.1016/j.cej.2016.04.079>
- Jin, Y.F., Zhang, Y.J., Zhang, Y.P., Chen, J., Zhou, X.M. and Bai, L.Y. (2013), “Synthesis and evaluation of molecularly imprinted polymer for the determination of the phthalate esters in the bottled beverages by HPLC”, *J. Chem.*, **2013**, 1-9. <https://doi.org/10.1155/2013/903210>
- Karsten, H. (2001), “Molecularly imprinted polymers in analytical chemistry”, *Analyst*, **126**, 747-756. <https://doi.org/10.1039/B102799A>
- Kenji, M., Yukihiko, A., Hong, Y., Kenji, O., Tetsuro, I., Toshiyuki, T., Emi, K., Monekazu, I. and Yoshinori, N. (2004), “Preferential target is mitochondria in  $\alpha$ -mangostin-induced apoptosis in human leukemia HL60 cells”, *Bioorg. Med. Chem.*, **12**(22), 5799-5806. <https://doi.org/10.1016/j.bmc.2004.08.034>
- María, del M.C.L., M.C. Cela, P., María, S.D.G., José, M.L.V., María, V.G.R. and Luis, F.B.L. (2012), “Preparation, evaluation and characterization of quercetin-molecularly imprinted polymer for preconcentration and clean-up of catechins”, *Anal. Chim. Acta*, **721**, 68-78. <https://doi.org/10.1016/j.aca.2012.01.049>
- Martín-Esteban, A. (2001), “Molecularly imprinted polymers: new molecular recognition materials for selective solid-phase extraction of organic compounds”, *Fresenius J. Anal. Chem.*, **370**, 795-802. <https://doi.org/10.1007/s002160100854>
- Martín-Esteban, A., Turiel, E. and Stevenson, D. (2001), “Effect of template size on the selectivity of molecularly imprinted polymers for phenylurea herbicides”, *Chromatographia*, **53**, S434-S437. <https://doi.org/10.1007/BF02490371>
- Mohamed, Y.I., Najihah, M.H., Abdalbasit, A.M., Syam, M., Mahmood, A.A., Siddig, I.A. and Ismail, A.A. (2016), “ $\alpha$ -Mangostin from *Garcinia mangostana* Linn: an updated review of its pharmacological properties”, *Arab. J. Chem.*, **9**(3), 317-329. <http://dx.doi.org/10.1016/j.arabjc.2014.02.011>
- Muchtaridi, M., Nadia, A.P., Tiana, M. and Ida, M. (2017), “Validation analysis methods of  $\alpha$ -mangostin,  $\gamma$ -mangostin and gartanin mixture in mangosteen (*Garcinia mangostana* L.) fruit rind extract from west java with HPLC”, *J. Appl. Pharm. Sci.*, **7**(10), 125-130. <https://doi.org/10.7324/JAPS.2017.71018>
- Nimibofa, A., Augustus, N.E. and Donbebe, W. (2017), “Modelling and interpretation of adsorption isotherms”, *J. Chem.*, **2017**, 1-11. <https://doi.org/10.1155/2017/3039817>
- Nor, A.Y., Siti, K.Ab.R., Mohd, Z.H. and Nor, A.I. (2013), “Preparation and characterization of molecularly imprinted polymer as SPE sorbent for melamine isolation”, *Polymers*, **5**(4), 1215-1228. <https://doi.org/10.3390/polym5041215>
- Pothitirat, W. and Gritsanapan, W. (2009), “HPLC quantitative analysis method for the determination of  $\alpha$ -mangostin in mangosteen fruit rind extract”, *Thai J. Agric. Sci.*, **42**(1), 7-12. <http://www.thaiscience.info/Journals/Article/TJAS/10469542.pdf>
- Qiao, F., Sun, H., Yan, H. and Row, K.H. (2006), “Molecularly imprinted polymers for solid phase extraction”, *Chromatographia*, **64**, 625-634. <https://doi.org/10.1365/s10337-006-0097-2>
- Robert, J.U., Sarah, C.B., Yizhao, C., Ripal, N.S. and Ken, D.S. (2001), “Characterization of molecularly imprinted polymers with the langmuir-freundlich isotherm”, *Anal. Chem.*, **73**(19), 4584-4591. <https://doi.org/10.1021/ac0105686>
- Tamayo, F.G., Turiel, E. and Martín-Esteban, A. (2007), “Molecularly imprinted polymers for solid-phase extraction and solid phase microextraction: recent developments and future trends”, *J. Chromatogr. A*, **1152**(1-2), 32-40. <https://doi.org/10.1016/j.chroma.2006.08.095>